Sriwijaya Journal of Environment
Article
ojs.pps.unsri.ac.id

Assessment of Groundwater Potential and Suitable Borehole Locations in Esan Central Using Remote Sensing and Geospatial Analysis

Stephen Olushola Oladosu*, Mabel Eghemenrior Alenkhe, Obehi Isesele, Tijjani Yusuf Muhammad

Department of Geomatics, Faculty of Environmental Sciences, University of Benin, P.M.B. 1154, Edo State, Nigeria.
**Corresponding Author*: olushola.oladosu@uniben.edu

Article history

Received	Received in revised form	Accepted	Available online
08 May 2025	20 June 2025	21 October 2025	30 December 2025

Abstract: Groundwater potential zone mapping is essential for identifying optimal sites for sustainable water infrastructure. This study presents a novel integration of ten environmental factors using remote sensing and GIS-based Analytical Hierarchy Process (AHP) to delineate groundwater potential zones and suitable borehole sites in Esan Central Local Government Area (LGA), Edo State, Nigeria. Unlike previous studies that focused on fewer variables, this research incorporates slope, geology, rainfall, drainage density, lineament density, land use/land cover, elevation, soil type, and proximity to infrastructure. The model was validated using 43 ground-truth locations with an overall accuracy of 85.3% and a Kappa coefficient of 0.78. Results showed that the majority of the area (65.2%) falls under moderate groundwater potential, while only 0.06% lies in the very high category. Borehole suitability analysis identified 43 optimal drilling locations. These findings provide actionable insights for planners and water agencies aiming to improve rural water access through scientifically grounded siting decisions.
Keywords: aquifer mapping; site suitability; water resources; spatial modeling; hydrogeology

1. Introduction

Groundwater is an essential resource for domestic, agricultural, and industrial use worldwide, particularly in regions facing water scarcity or limited access to surface water. In Southeast Asia and the Pacific, for instance, groundwater contributes significantly to drinking water supply, although challenges such as over-abstraction and contamination persist [1]. Similarly, in Nigeria, the strategic management of groundwater is increasingly vital for achieving sustainable agricultural irrigation and water security in rural and peri-urban areas [2]. As global attention intensifies on achieving Sustainable Development Goals (SDGs), groundwater has emerged as a pivotal asset in realizing SDG 6, clean water and sanitation for all [3]; [4]; [5]; [6]; [7].

However, the spatial variability of groundwater occurrence, especially in fractured basement terrains, complicates its exploration and sustainable exploitation [8]; [9]. In arid and semi-arid environments such as Somalia, hydrogeological complexities, coupled with limited field-based data, hinder effective groundwater development [10]. In Nigeria and many other African countries, the dearth of comprehensive aquifer maps and real-time monitoring infrastructure underscores the need for geospatial and multi-criteria approaches to groundwater potential zoning (GWZ).

Remote sensing and Geographic Information Systems (GIS), integrated with Multi-Criteria Decision-Making (MCDM) tools like the Analytic Hierarchy Process (AHP) [11], [12], [13], [14] have been widely adopted to assess groundwater potential. AHP enables assigning weights to thematic layers based on expert judgment or empirical validation [15]; [16]. While these methodologies have gained global traction, their contextual adaptation in West Africa has often suffered from methodological inconsistencies, limited spatial coverage, and weak integration of hydrogeological variables [17]; [18].

A mini-meta-analysis of relevant studies in West Africa reveals diverse methodological approaches and varying performances of AHP-based models. For example, [8]; [9] combined AHP, hydro geophysical and remote sensing data to delineate groundwater potential in West-Africa, this demonstrated the significance of geoelectric parameters in refining aquifer zoning. In Lapan Gwari, Nigeria, [12] employed a combination of remote sensing and electrical resistivity sounding to identify high-potential zones, showing the synergy of surface and subsurface data integration [13]. [10], in Somalia, applied Electrical Resistivity Tomography (ERT) and revealed the value of stratigraphic profiling in arid hydrogeological modeling. [19] further highlighted the potential of integrated resistivity and remote sensing in North-West Nigeria, which reinforces the reproducibility of such approaches in basement terrains.

Despite these advances, key gaps persist. First, there is a lack of standardized frameworks that allow for cross-site comparisons or regional-scale synthesis. Second, many existing studies neglect crucial variables such as recharge rate, lithology, and groundwater abstraction intensity [20]; [21]. Finally, while several studies apply the AHP technique, few validate the resulting GWZ maps against borehole yield data or

field surveys, leading to uncertainties in model accuracy and policy relevance.

This study, therefore, aims to fill these gaps by implementing an AHP-GIS framework for groundwater potential mapping in Esan Central, a region characterized by complex geology and growing water demand. The scientific contribution lies in the development of a validated, multi-parameter GWZ model that integrates both surface, such as land use, slope, drainage density, and subsurface, such as lithology, lineament density, and aquifer resistivity datasets. The approach not only refines methodological consistency but also provides a replicable framework for other parts of West Africa.

By situating the study within a broader regional context and synthesizing emerging methodologies, this research bridges the divide between academic modeling and real-world groundwater planning. Ultimately, the findings are expected to support data-driven decision-making for water resource management and infrastructure development in Esan Central and similar hydrogeological environments.

2. Materials and Methods

2.1 Study area

Esan Central Local Government Area (LGA) is situated within Edo State, Nigeria, specifically in the southeastern part. It forms part of the Esanland region, renowned for its rich cultural heritage and historical significance. Covering an area of 253 square kilometers, it sustains a population density of 545.1 individuals per square kilometer. Similar to other LGAs in Nigeria, Esan Central is subdivided into wards and villages, each characterized by distinct features and community dynamics. Local government administration plays a pivotal role in steering the area's development and governance. Positioned between Latitude 6°41'3.94"N to 6°55'48.49"N and Longitude 6°13'6.88"E to 6°18'16.59"E, Esan Central LGA grapples with challenges common to many regions, including infrastructure development, healthcare accessibility, and economic diversification. Collaborative efforts involving the local government, community organizations, and individuals strive to mitigate these challenges and foster sustainable development. Figure 1 depicts the map of the study area.

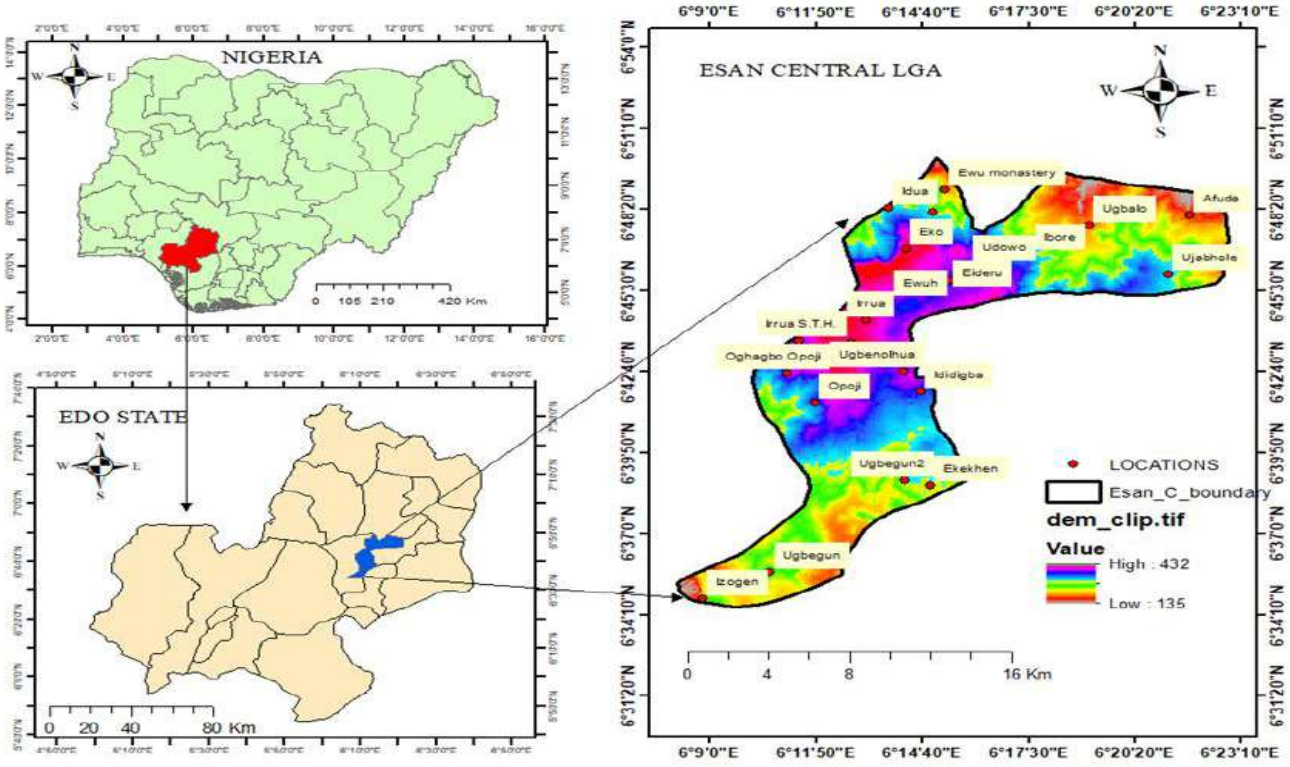

Figure 1. Map of the Study Area

2.2 Methods

To delineate groundwater potential and borehole suitability, GIS and RS techniques were applied. This was done in the Esan Central LGA, Edo state in Nigeria through an analytical hierarchy process. Methods for this research work include the identification and evaluation of criteria, data collection, preprocessing, input data set, reclassified input layers, pairwise comparison of criteria and weighting with the hierarchical analytical process (AHP), overlay analysis with weight sum overlay analysis in ArcGIS tools, and final value ranking. The overall methods are shown as shown in Figure 2.

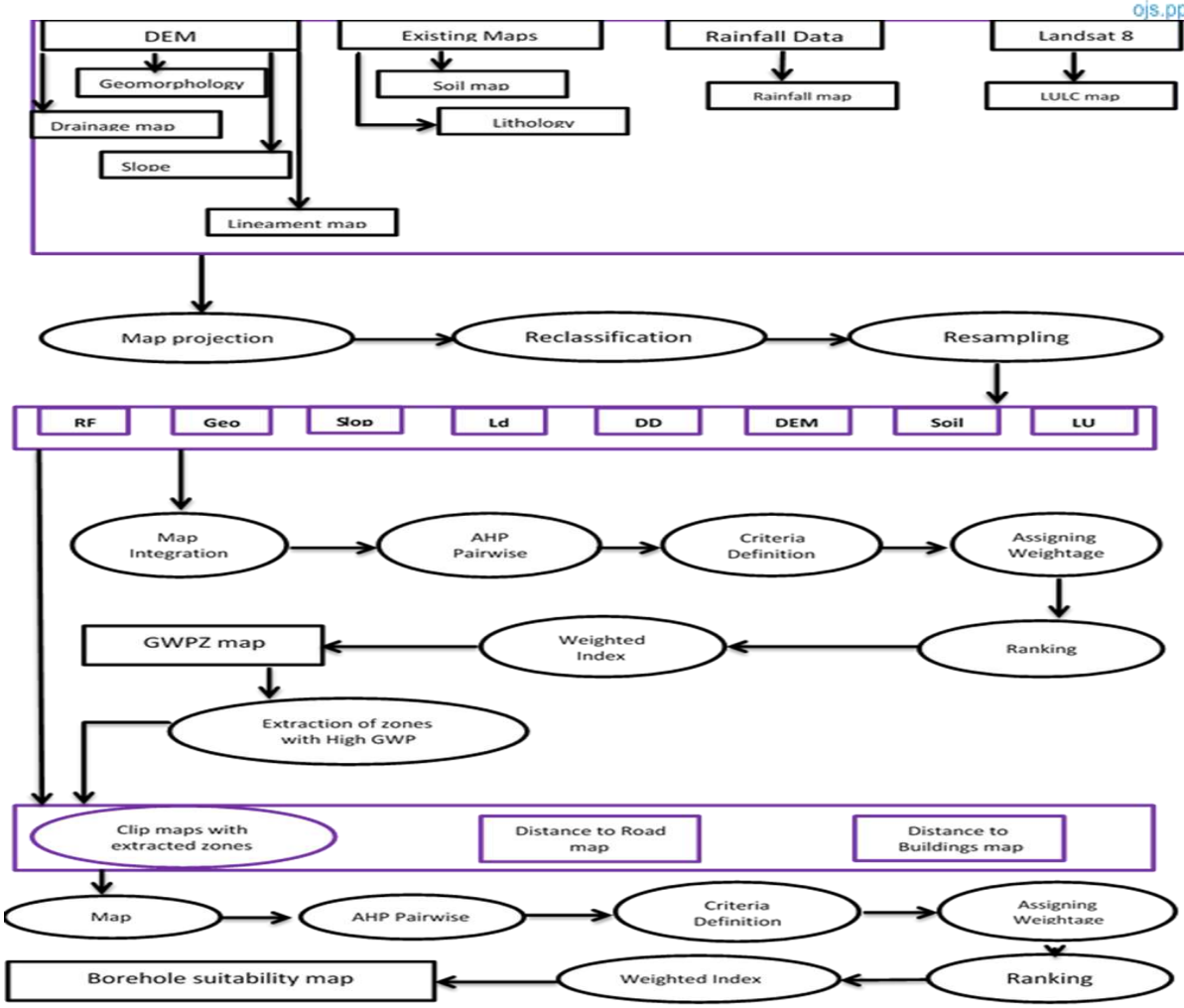

Figure 2: Diagram Showing the Study Procedures Adapted from [19]

2.3 Materials

2.3.1 Data Source and Description

The data used for both groundwater potential zone mapping and borehole suitability mapping were sourced from various reputable platforms. The CRU Climate website provided rainfall data validated with Nigeria metrological (NIMET) rainfall data locally, which was crucial for evaluating groundwater recharge potential. Geological data and Digital Elevation Model (DEM) information, including topography and groundwater movement patterns, were obtained from the USGS website. The FAO website contributed soil data, which was essential for assessing infiltration capacity. The shapefiles for buildings and roads were obtained from the Diva GIS website, and were instrumental in borehole proximity calculation. These datasets form the foundation for the mapping efforts. Table 1. Shows the data information summary.

2.3.2 Production of Thematic Maps

The input layers for the study were prepared to account for multiple variables, including thematic maps of rainfall, geology, lineaments, elevation, slope, drainage, land use/land cover, and soil. These maps were generated primarily through satellite imagery using digital image processing techniques and existing data sources. During the GIS spatial database creation, the collected data were digitized manually using ArcGIS 10.4 software at various scales sourced from different organizations.

Table 1. Summary of data acquisition and information.

S/N	Data	Purpose	Source
1	Rainfall	To evaluate GW recharge in conjunction with RF	CRU climate website/NIMET
2	Geological data	GW movement	USGS website
3	DEM	To generate; slop, drainage density, lineament density	USGS website
4	Soil data	Infiltration capacity	FAO website
5	Landsat 8	Permeability rainfall	USGS website
6	Buildings and Roads shapefile	To calculate borehole proximity	Diva GIS website

The thematic maps included elevation, slope, soil, land use/land cover, lithology, drainage, rainfall, and lineament maps. Current geology, soil, land use/land cover, and lineament data in shapefile ('shp') format were converted to raster format using the polygon-to-raster tool, applying a cell size of 30 x 30 meters. This

cell size was also used to construct maps for drainage density and slope. The project tool in ArcGIS was used to re-project all maps into a uniform coordinate system. The lineament map was further processed into a lineament density map (km/km²) using the line density tool within the spatial analysis suite. Weights ranging from 1 to 5 were assigned to each parameter based on its relative contribution to the study.

For borehole suitability mapping, the set null and less-than tools were applied to isolated areas with high groundwater potential. The selected areas were converted into shapefiles (polygons) through rigorous supervision and used to clip slope, geology, soil, and elevation maps. Distance-to-road and distance-to-building maps were created using downloaded shapefiles and the Euclidean distance tool, ensuring the suitability mapping considered accessibility and proximity to infrastructure.

Table 2. Summary of criterial groundwater and borehole suitability mapping

Key Factor	Significance	Equation/Method
Drainage Density	Indicates surface runoff and infiltration potential. Low density suggests higher recharge rates.	$D_d = \frac{\text{Total length of straeam}}{\text{Area}}$
Rainfall	Serves as a primary source for groundwater recharge. Higher rainfall indicates better recharge potential.	Use rainfall intensity maps or R_i = P x t (where P is the precipitation, t is the time).
Lineament Density	Identifies subsurface geological formations affecting groundwater flow, such as faults and fractures.	$L_d = \frac{\text{Total length of lineaments}}{\text{Area}}$
Land Use/ Land Cover	Reflects surface conditions affecting recharge. Vegetation enhances infiltration, while urbanization hinders it.	Classification through GIS and supervised/unsupervised classification techniques.
Geology	Determines aquifer properties like permeability and storage capacity.	Analysis of lithology through geological maps and GIS overlays.
Soil	Influences permeability and porosity, crucial for water movement and storage.	$P_e = \frac{K_s}{\eta}$ (where K_s is the saturated hydraulic conductivity, η is the porosity).
Geomorphology	Highlights terrain features influencing groundwater distribution and recharge.	GIS-based classification of geomorphological units.
Slope	Controls water infiltration and runoff. Gentle slopes promote recharge, while steep slopes hinder it.	$S = \tan^{-1}\left(\frac{\Delta h}{d}\right)$ (where Δh is the elevation change, d is the distance).
Distance to Road Network	Facilitates drilling, maintenance, and water distribution.	Buffer analysis in GIS to determine proximity zones.
Distance to Residential Areas	Ensures accessibility and convenience for users.	Buffer analysis in GIS based on population distribution.
Elevation	Affects borehole stability and cost. Higher elevations may require advanced drilling; lower elevations risk flooding.	Digital Elevation Model (DEM) analysis through GIS.

2.4. Prevailing Criteria for Groundwater Potential Zone and Borehole Suitability Mapping

Table 2 is a representation of the factors, their significance, and the equations or methods used for evaluation in groundwater potential zone and borehole suitability mapping.

2.5 The Analytical Hierarchy Process and Multicriteria Evaluation

The original formulation by Saaty [13] used a scale of 1 to 9 to represent the relative importance of factors, where a_{ij} is the relative importance of factor *i* to factor *j*. The Analytical Hierarchy Process serves as a decision support tool designed to assist users in making optimal decisions, particularly in complex scenarios. Its hierarchical framework comprises goals, criteria for decision-making, and potential options [12]; [13]; [22]. It facilitates the conversion of both quantitative measurements like cost and weight, and qualitative judgments like pleasure and preference, into inputs.

In AHP, Satty's scale, a verbal scale, is employed to enable decision makers to naturally integrate subjectivity, experience, and knowledge [12]; [13]; [23]. Equations 1-6 summarize the basic computation involved in the AHP process while Tables 3 and 4 show the Intensity of Relative Importance and the normalized vector representation.

$$\begin{bmatrix} a_{11} & a_{12} & \text{L} & a_{1n} \\ a_{21} & a_{22} & \text{L} & a_{2n} \\ \text{M} & \text{M} & \text{O} & \text{M} \\ a_{n1} & a_{n2} & \text{L} & a_{nn} \end{bmatrix} \quad \text{..... (1)}$$

Where: $a_{ij} = \frac{1}{a_{ji}}$, and $a_{ii} = 1$

Normalization is performed using equation 2 as follows.

$$\begin{bmatrix} \frac{a_{11}}{\sum_{k=1}^{n} a_{k1}} & \frac{a_{12}}{\sum_{k=1}^{n} a_{k2}} & \text{L} & \frac{a_{1n}}{\sum_{k=1}^{n} a_{kn}} \\ \frac{a_{21}}{\sum_{k=1}^{n} a_{k1}} & \frac{a_{22}}{\sum_{k=1}^{n} a_{k2}} & \text{L} & \frac{a_{2n}}{\sum_{k=1}^{n} a_{kn}} \\ \text{M} & \text{M} & \text{O} & \text{M} \\ \frac{a_{n1}}{\sum_{k=1}^{n} a_{k1}} & \frac{a_{n2}}{\sum_{k=1}^{n} a_{k2}} & \text{L} & \frac{a_{nn}}{\sum_{k=1}^{n} a_{kn}} \end{bmatrix}; \text{..... (2)}$$

in a simplified form $n_{ij} = \frac{a_{ij}}{\sum_{k=1}^{n} a_{kj}}$

Compute the weight w_i using equation 3

$$w_{ij} = \frac{\sum_{j=1}^{n} a_{ij}}{n}; \text{ in matrix form, } w = \begin{bmatrix} w_1 \\ w_2 \\ \text{M} \\ w_n \end{bmatrix}$$

……..(3)

Compute the consistency index following the steps presented in equation 4

$$\left.\begin{array}{l} \text{Compute the weighted sum vector}: WS_i = \sum_{j=1}^{n} a_{ij} \times w_j \\ \text{Calculate the consistency vector}: \lambda_i = \frac{WS_i}{w_i} \\ \text{Determine the largest eigenvalue}: \lambda_{\max} = \frac{\sum_{i=1}^{n} \lambda_i}{n} \\ \text{Compute the consistency index}: CI = \frac{\lambda_{\max} - n}{n-1} \end{array}\right\}$$

..(4)

Compute the consistency index using equation 5

$$CI = \frac{\lambda_{\max} - n}{n-1} \text{ ……...(5)}$$

The Consistency Ratio (CR) checks the reliability of the weights:

$$CR = \frac{CI}{RI} \text{ .....(6)}$$

Where: RI is the Random Index for a given n (from a standard table). If CR<0.10, the pairwise comparison matrix is consistent.

Table 3. Saatty's scale of relative importance

The Intensity of Relative Importance	Definition of how important
1	Equal importance
2	Weak or slight importance
3	Moderate importance
4	Moderate plus
5	Strong importance
6	Strong plus
7	Very strong
8	Very, very strong
9	Extremely importance

Table 4. Various numbers of factors and their corresponding random index

Number of Factor (n)	Random Index (RI)	Number of Factor (n)	Random Index (RI)	Number of Factor (n)	Random Index (RI)
1	0.00	6	1.24	11	1.51
2	0.00	7	1.32	12	1.48
3	0.58	8	1.41	13	1.56
4	0.90	9	1.45	13	1.57
5	1.12	10	1.49	15	1.59

2.6 Assignment of Ranks and Reclassification

From Saaty's method, reclassifying of ranks used in the AHP used in this work involves assigning numerical values to qualitative judgments to create a pairwise comparison matrix [12]; [13]; [24]. The scale proposed in Table 5 is a modified logic scale approach of assigning a weight to each polygon of each theme to make the process easier and more intuitive.

2.7. Suitability Model

A suitability model allocates weights to different locations based on pre-established criteria to assess their suitability for specific purposes. As outlined by Wade and Sommer in the A to Z Geographic Information System, these models serve to pinpoint optimal sites for various purposes, including new constructions, road placements, or habitats for specific species, as shown in equation 7 [25][26].

$$S = \sum_{i=1}^{n} w_i \times C_i \text{ .....(7)}$$

Where: S is the suitability score for the location, w_i weight of criterion i, C_i is the standardized score of criterion i, n is the total number of criteria.

Table 5. Simplified Saaty's scale to a 1–5 ranking system

Intensity of Importance	Definition	Explanation
1	Equal Importance	Two themes contribute equally to the objective of the problem at hand.
2	Slightly More Important	One theme is marginally preferred over the other based on judgment or evidence.
3	Moderately More Important	One theme is clearly more important, but not overwhelmingly so.
4	Strongly More Important	One theme is significantly more important and dominates in most considerations.
5	Extremely More Important	One theme is absolutely critical, and the other has little to no impact on the objective.

2.8. Ground Truthing

Validation was conducted using 43 georeferenced ground control points collected with handheld GPS devices. These points represent both functional and non-functional boreholes, wells, and spring locations across Esan Central LGA. Each was cross-checked with the predicted groundwater potential zones. A confusion matrix was generated by comparing observed borehole success with model-predicted suitability. This yielded an overall accuracy of 85.3% and a Cohen's Kappa coefficient (κ) of 0.78, indicating substantial agreement beyond random chance. Although ROC curves are more appropriate for continuous classification outputs, the discrete classification in this study made the Kappa statistic more suitable for assessing agreement [27].

3. Results and Discussion

3.1 Results for groundwater potential zone mapping.

All maps produced are in the WGS84 UTM Zone 32 N coordinate system on a scale of 1:170,000.

3.1.1 Rainfall

Rainfall emerged as the most influential factor for groundwater recharge, as reflected in its highest weight (32.46%) in the AHP model. The southern part of Esan Central LGA, characterized by rainfall above 1,933 mm/year, exhibits optimal conditions for aquifer recharge due to sustained moisture availability. This corresponds with areas delineated as very high groundwater potential zones. In contrast, the northern zones receive less than 1,801 mm annually, indicating lower infiltration potential and hence a greater risk of groundwater scarcity. These spatial rainfall differences play a foundational role in groundwater sustainability planning, as shown in Figure 3.

3.1.2 Drainage Density

Drainage density Figure 4 serves as a proxy for surface runoff and infiltration behavior. Areas with very low drainage density, primarily in the southeastern portion of the study area, are indicative of limited runoff and greater infiltration capacity, making them favorable for groundwater recharge. Conversely, the high drainage density observed in central and northern regions points to increased surface runoff and poor infiltration, reducing groundwater potential despite moderate rainfall in those areas. Thus, drainage patterns reinforce spatial variability in recharge capacity.

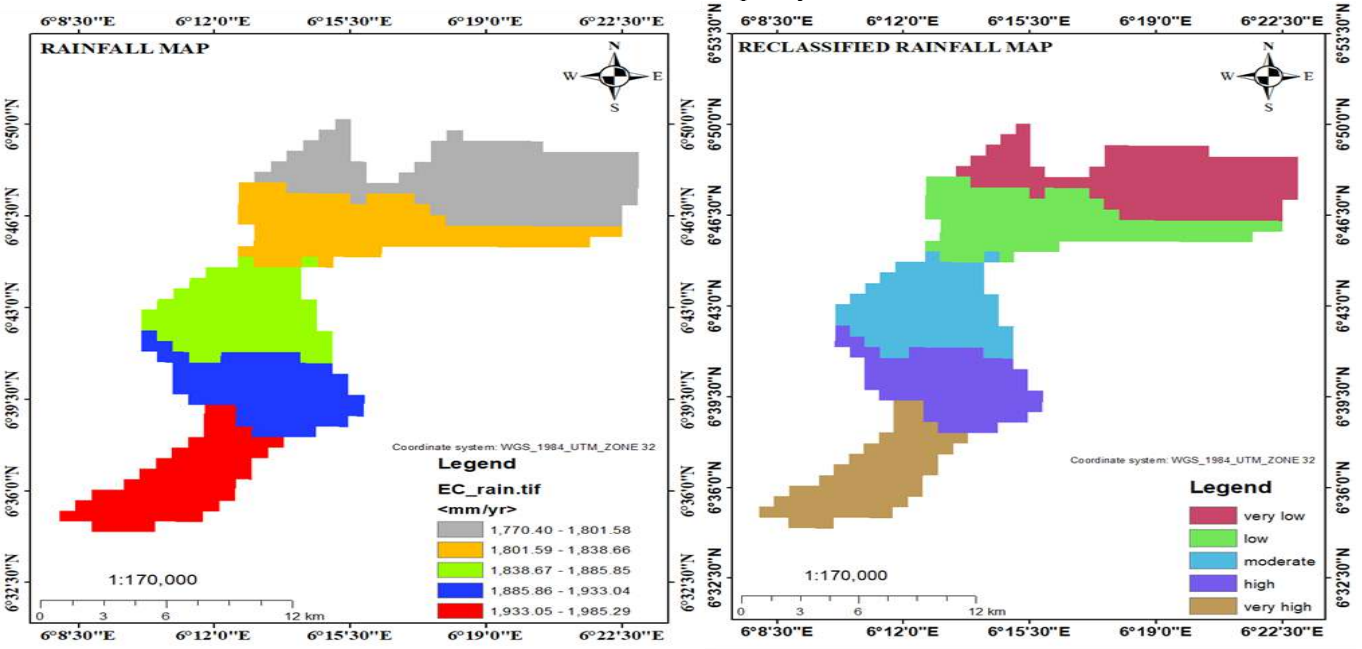

Figure 3. Rainfall Map and Reclassified Rainfall Map

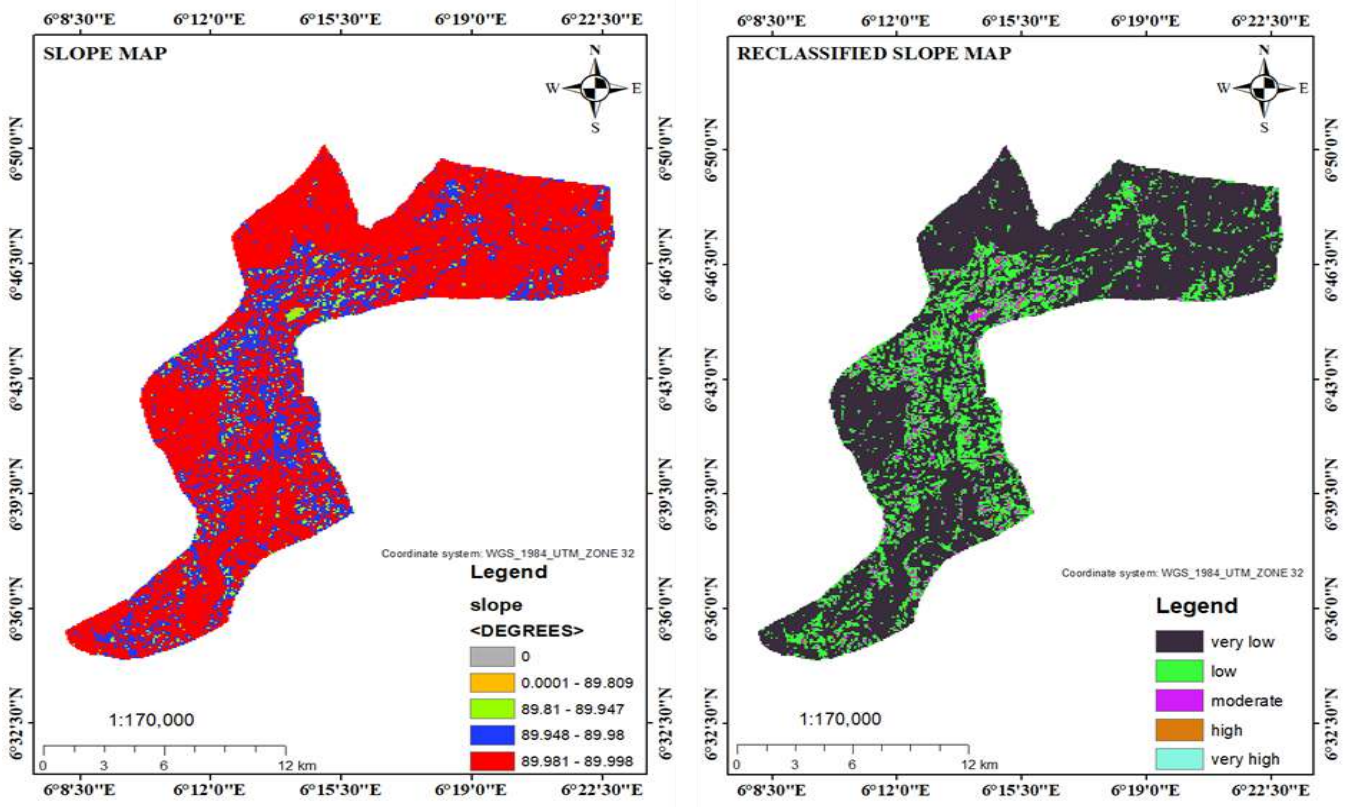

Figure 4. Drainage Density Map, Reclassified Drainage Density Map

3.1.3 Slope

Slope strongly influences groundwater infiltration by controlling surface runoff rates. The flat terrains (0°) received the highest suitability weight (5), indicating very high infiltration potential. These flat to gentle slopes dominate the southwestern and central regions of the study area, facilitating better infiltration and recharge due to slower water movement. In contrast, steep (89.948°–89.98°) and very steep slopes (89.981°–89.998°), with weights of 2 and 1, respectively, are concentrated in the northeast and are associated with high runoff and minimal recharge potential. This supports the inverse relationship between slope and groundwater suitability.

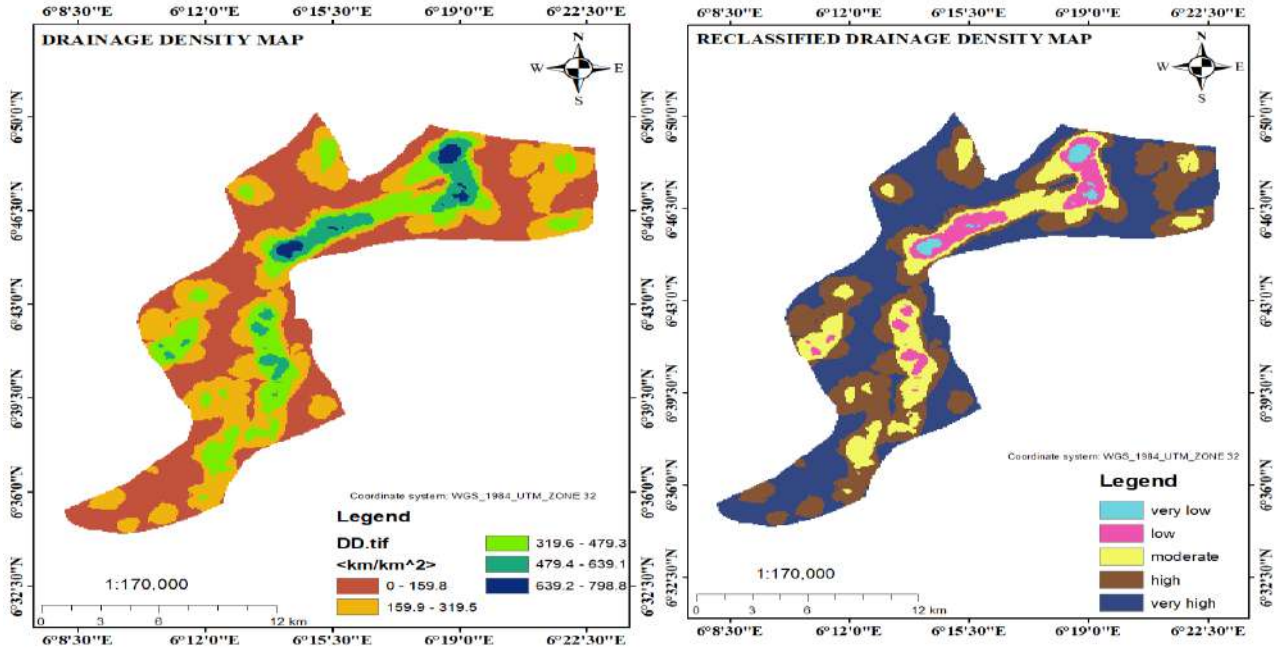

Figure 5: Slope Map, Reclassified Slope Map

3.1.4 Lineament Density

The lineaments within the study area exhibited orientations predominantly aligned with the directions of tributaries and wetlands, indicating a correlation between aquifer directions and surface water bodies. Lineament density analysis was conducted using ArcGIS tools and categorized into nine classes: 0 – 20.6, 20.7− 41.3, 41.4− 61.9, 62 – 82.6, 82.7 – 103, 104 – 124, 125 – 145, 146 – 165, 166 - 186 km/km^2. Lineament density reflects structural features that influence subsurface water flow. As presented in Figure 6, areas with the highest lineament density (146–186 km/km^2) were assigned a suitability weight of 5, indicative of very high infiltration potential due to increased fracture connectivity. These regions, primarily in the central and southern areas, align with zones of high groundwater recharge. Conversely, regions with the lowest density (0–20.6 km/km^2) received a weight of 1, marking them as the least favorable for groundwater accumulation.

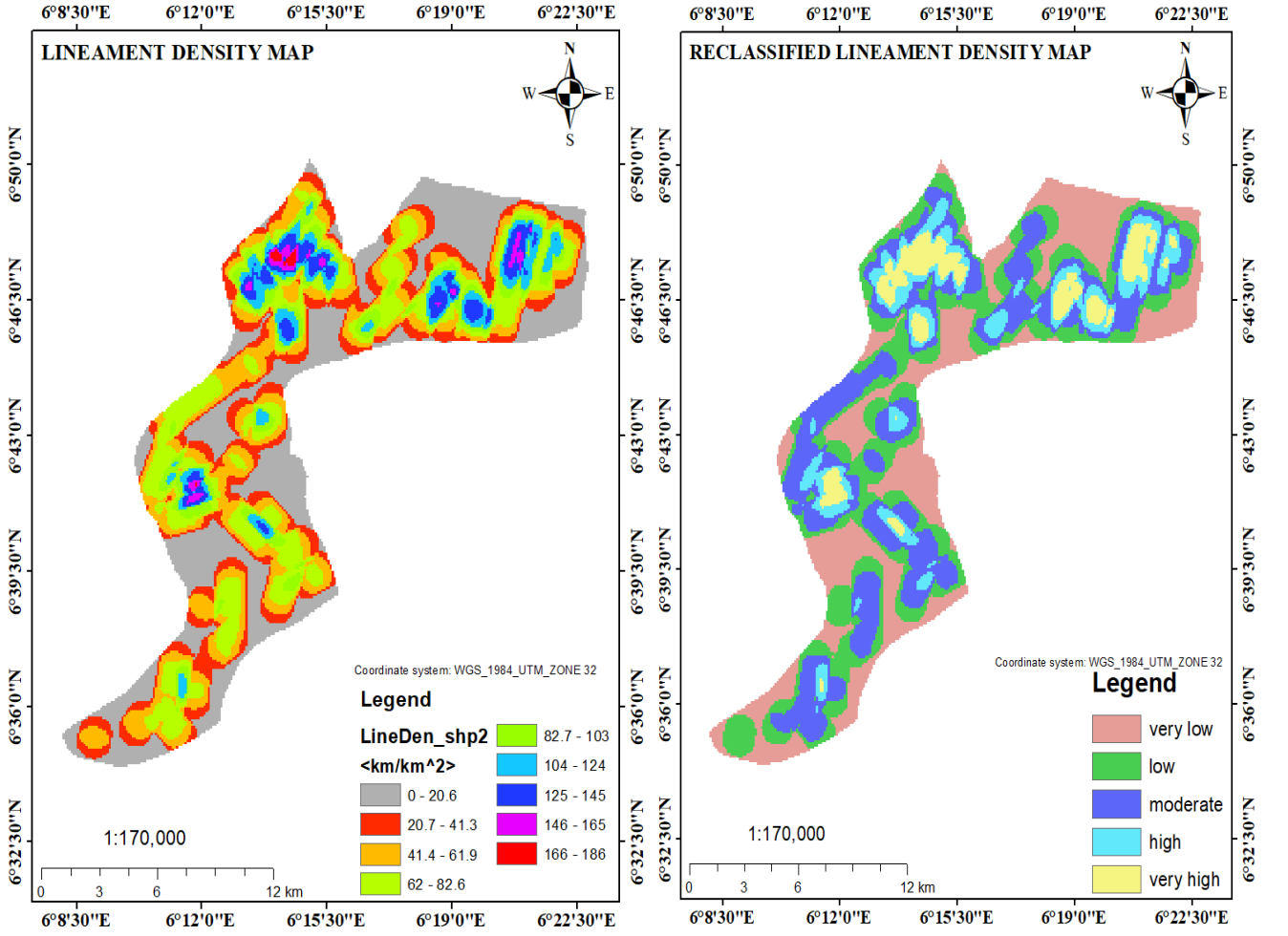

Figure 6: Lineament Density Map, Reclassified Lineament Density Map

3.1.5. Soil Texture

The soil texture of the study area was reclassified into two classes based on FAO 1998 guidelines, namely sandy clay and clay loam. These soil types were further described in terms of their hydrological soil group (HSG) properties according to the Universal Soil Data Analysis (USDA).

Soil type significantly influences infiltration rates and water retention. The soil classification indicates that sandy clay soils, with infiltration rates of 20–30 mm/hr, were given the highest weight (5), reflecting their high permeability and suitability for recharge. These dominate the southern parts of the study area. In contrast, clay loam soils (5–10 mm/hr), with a lower weight of 1, are mostly found in the north-central zone and present lower infiltration potential. This spatial variation contributes to differences in groundwater potential. These rates were then reclassified to indicate suitability for groundwater potential, as depicted in Figure 7.

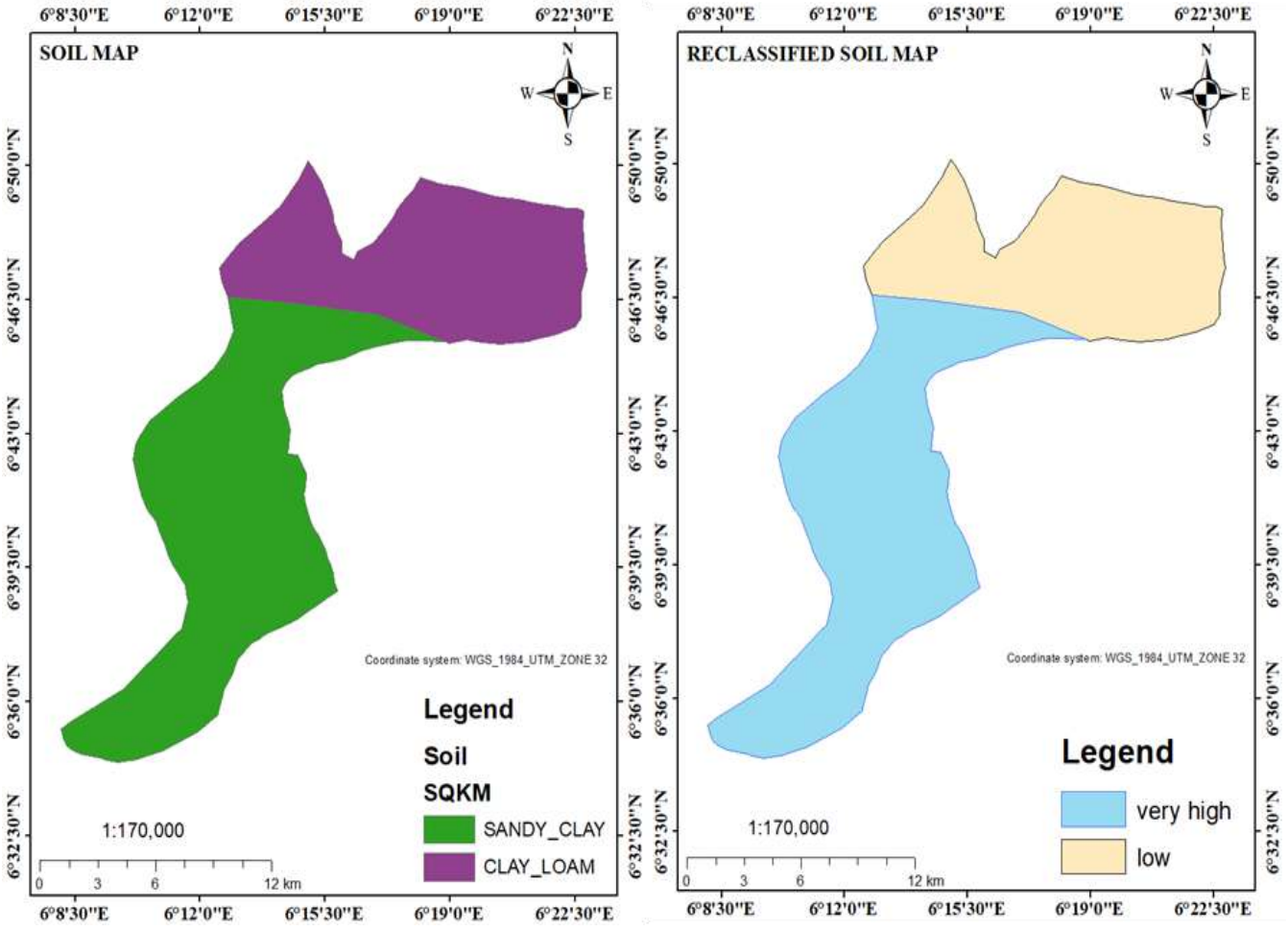

Figure 7: Soil Map, Reclassified Soil Map

3.1.6. Land-Use/Land-Cover Suitability

Land-use/land-cover significantly influences hydrological processes such as surface runoff, evapotranspiration, and groundwater recharge. Water bodies, forested areas, and vegetation are identified as excellent groundwater sources and contribute significantly to recharge. In contrast, bare lands and built-up areas have a lesser impact on groundwater recharge, as indicated in Figure 8, which revealed the land use land cover type and the reclassified LULC around the study area.

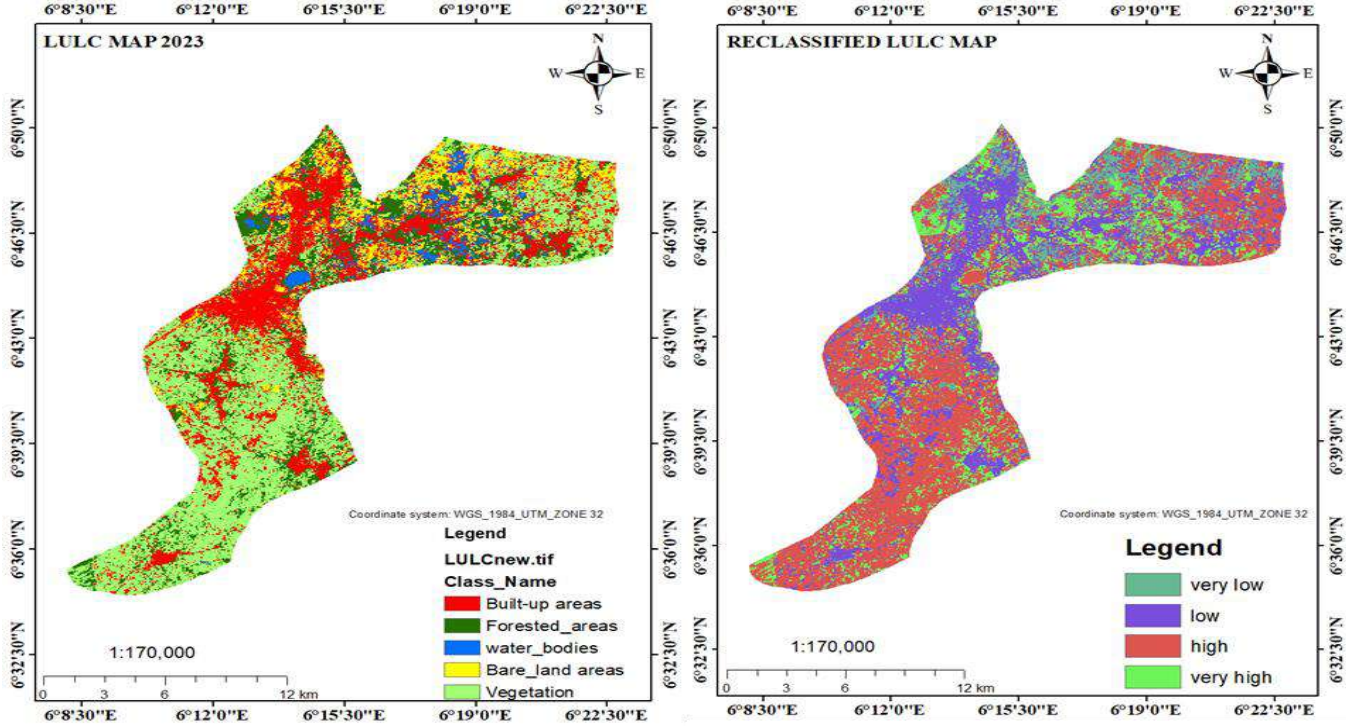

Figure 8: Land Use Land Cover Map, Reclassified Land Use Land Cover Map

3.1.7: Digital Elevation and Surface Analysis Suitability

The present study utilized Shuttle Radar Topographic Mission (SRTM) elevation data with a resolution of 30 m × 30 m to acquire surface data. This elevation data was processed using remote sensing and GIS software, specifically ArcGIS 10.4, to generate a Digital Elevation Model (DEM), slope, and aspect maps. The characteristics of the DEM showed that the highest elevation recorded was 432 m, while the lowest elevation was 135 m. Consequently, the majority of the study area was covered by high elevations, suggesting a lower likelihood of groundwater presence. Figure 9 represents the DEM and reclassified DEM maps.

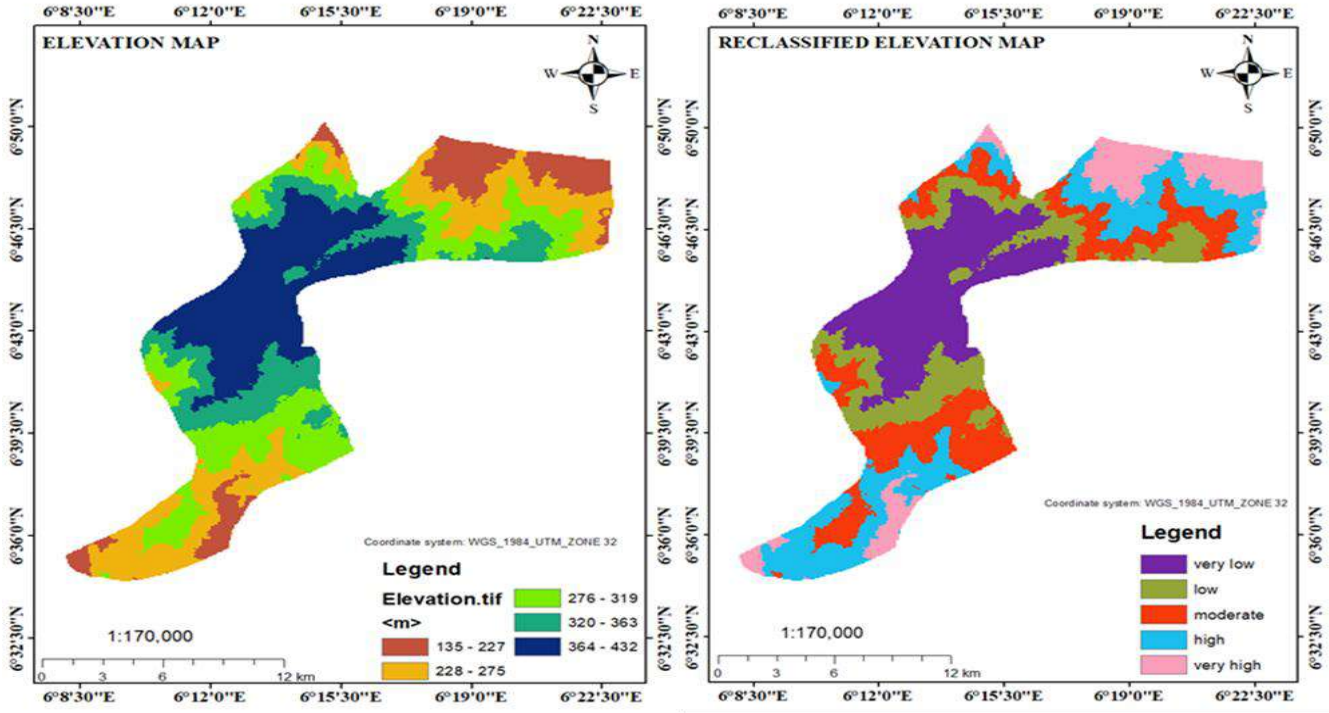

Figure 9: Elevation Map, Reclassified Elevation Map

3.1.8: Geological Map Suitability

The lithological stratigraphy of the Esan Central Local Government Area was sourced from the USGS site and investigated by the United States Geological Survey. The study area primarily comprises tertiary rock units, with the Quartinery Tertiary group (QT) being predominant, followed by Cretaceous, Cenozoic, and Holocene deposits, mostly in small mounds or linear domes.

Each lithological unit was reclassified based on its groundwater recharge potential into categories such as very high, moderate, low, and very low. Figure 10 illustrates the distribution of rock types in the study area. However, it's important to note that while these lithological units exist, they do not all hold equal significance in determining and controlling groundwater

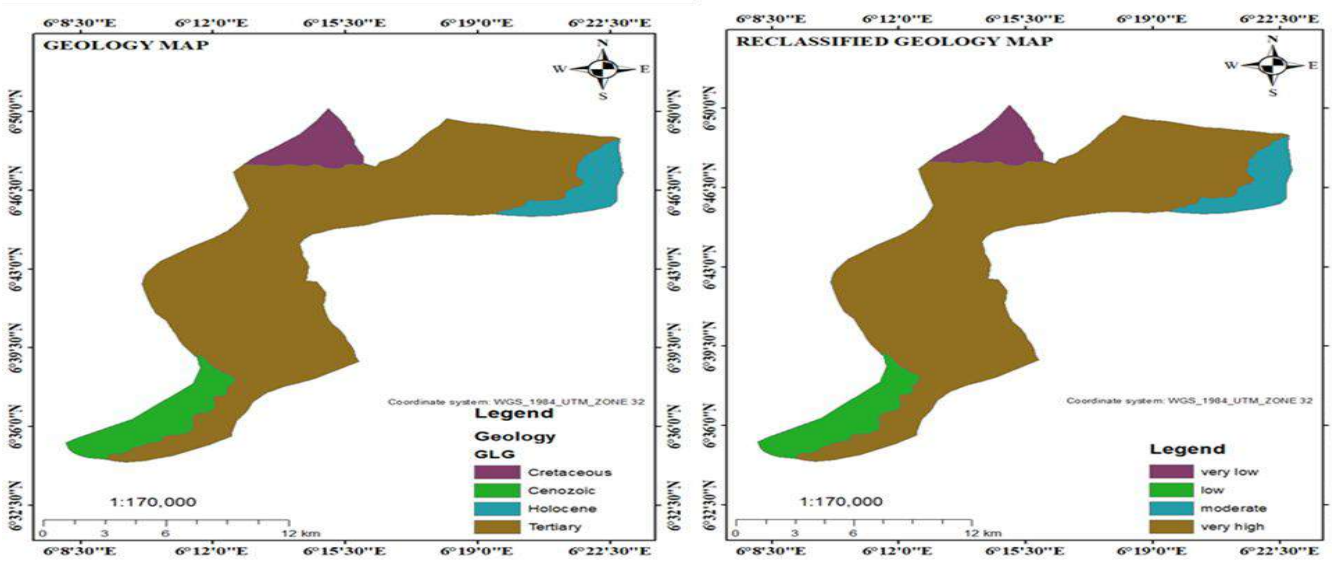

Figure 10: Geological Map, Reclassified Geological Map

3.2. Mapping Groundwater Potential Zone

The successful integration of all the thematic maps enabled an output raster map to be obtained. Moreover, that map shows the potential groundwater zones. Earlier, ranks from 1 to 5 were assigned for individual classes of rainfall, geology, DEM, slope, soil, land use/ land cover, drainage density, and lineament density layers based on the influence on groundwater potential and recharge zone. Hence, the final output map was also obtained with 5 classes. As per the rank assignment, value 5 indicates a very high groundwater potential area, 4 indicates a high groundwater potential, 3 indicates a moderate groundwater potential area, 2 indicates a low groundwater potential area, and 1 indicates a very low groundwater potential area. Table 6 shows the criteria used in the ranking of the groundwater potential zone analysis, while Table 7 contains the results of the normalization of the criteria.

Table 6: Ranking of groundwater potential zone analysis criteria.

Parameter	RF	Geo	Slop	LD	DD	DEM	Soil	LULC
RF	1	2	3	5	6	4	6	7
Geo	0.5	1	2	3	5	5	6	7
Slop	0.33	0.5	1	0.5	2	4	2	3
LD	0.2	0.33	2	1	1	2	2	3
DD	0.16	0.2	0.5	1	1	2	3	4
DEM	0.25	0.2	0.25	0.5	0.5	1	3	4
Soil	0.167	0.167	0.5	0.5	0.33	0.333	1	4
LULC	0.14	0.143	0.33	0.33	0.25	0.25	0.25	1
Total	2.76	4.543	9.58	11.8	16.08	18.583	23.25	33

Table 7: Normalizing the criteria columns to obtain the normalized matrix.

Parameter	RF	Geo	Slop	LD	DD	DEM	Soil	LULC	Weight	(%)
RF	0.362	0.440	0.313	0.422	0.374	0.215	0.258	0.212	0.324	32.458
Geo	0.181	0.220	0.209	0.253	0.311	0.270	0.258	0.212	0.239	23.920
Slop	0.121	0.111	0.104	0.042	0.124	0.215	0.086	0.090	0.111	11.173
LD	0.073	0.073	0.209	0.085	0.062	0.107	0.086	0.090	0.098	9.821
DD	0.061	0.044	0.052	0.085	0.062	0.108	0.129	0.121	0.082	8.265
DEM	0.091	0.044	0.027	0.042	0.032	0.054	0.129	0.121	0.067	6.726
Soil	0.061	0.037	0.052	0.042	0.021	0.018	0.043	0.121	0.049	4.931
LULC	0.052	0.031	0.035	0.028	0.016	0.013	0.010	0.030	0.027	2.702

3.2.1 Weight Normalization

The weights were normalized as depicted in Table 7. This involved averaging the values in each row to derive the corresponding rankings, thereby obtaining the normalized weights for each parameter. The findings reveal that observed rainfall has the highest value compared to the other parameters. This implies that higher rainfall is likely to lead to greater groundwater recharge, resulting in higher groundwater potential zones. Conversely, lower rainfall suggests reduced groundwater recharge and thus lower groundwater potential zones.

3.2.2 Principal Eigen Vector

To confirm the weights assigned to each parameter in Table 7, the normalized principal eigenvector value (λ_{max}) was determined to assess the consistency ratio. This process entailed multiplying the weight of each criterion, like rainfall (as illustrated in Table 8), by the corresponding total value from the pairwise comparison matrix (e.g., Rainfall was 2.868 in Table 8). Adding up these products gives the consistency vector (λ_{max} = 8.9), as depicted in Table 9, which is utilized to compute the consistency index. The consistency index (CI) was then calculated to establish the consistency ratio formula, resulting in CI = 0.08. Subsequently, the consistency ratio (CR) was computed, resulting in CR = 0.057, which is below 0.1, indicating that the assigned weights were suitable for further analysis (Table 9). Groundwater potential zone map (GWPZM) was computed after checking all criteria by multiplying all reclassified conditioning factors by their calculated weight percentage.

Following the successful integration of all thematic maps, an output raster map was generated to depict potential groundwater zones. Previously, ranks ranging from 1 to 5 were assigned to individual classes of rainfall, geology, elevation, slope, soil, land use/land cover, drainage density, and lineament density layers, based on their influence on groundwater potential and recharge zones. Consequently, the final output map was categorized into 4 classes.

In this classification scheme, a value of 5 indicates a very high groundwater potential area, 4 indicates high potential, 3 indicates moderate potential, 2 indicates low potential, and 1 indicates very low potential, as demonstrated in all the reclassified maps. Rainfall was given a higher weight than other parameters, as it has a greater influence on groundwater potential and recharge zones. The groundwater potential zones were delineated into very high, high, moderate, and low categories, as illustrated in Figure 11.

Table 8: Calculating the Consistency of the criteria columns to obtain the λ_{max}.

Consistency Matrix											
Parameter	RF	Geo	Slop	LD	DD	DEM	Soil	LULC	Weighted sum	Criteria Weight	Total
RF	0.324	0.478	0.333	0.49	0.492	0.268	0.294	0.189	2.868	0.324	8.9
Geo	0.162	0.239	0.222	0.294	0.41	0.335	0.294	0.189	2.145	0.239	8.9
Slop	0.107	0.119	0.111	0.049	0.164	0.268	0.098	0.081	0.997	0.111	8.9
LD	0.065	0.079	0.222	0.098	0.082	0.134	0.098	0.081	0.859	0.098	8.7
DD	0.052	0.048	0.056	0.098	0.082	0.134	0.147	0.108	0.725	0.082	8.8
DEM	0.081	0.048	0.028	0.049	0.041	0.067	0.147	0.108	0.569	0.067	8.4
Soil	0.054	0.039	0.056	0.049	0.027	0.022	0.049	0.108	0.404	0.049	8.2
LULC	0.045	0.034	0.037	0.032	0.021	0.017	0.012	0.027	0.225	0.027	8.3

Table 9: Random Index and consistency ratio (GWPZM)

N		**8**
λ_{max}	$\frac{(8.9+8.9+8.9+8.7+8.8+8.4+8.2+8.3)}{8}$	8.6
CI	$\frac{(\lambda_{max}-n)}{n-1}$ $\frac{(8.6-8)}{8-1}=\frac{0.6}{7}=0.085$	0.08
RI		1.41
CR	CI/RI	0.057
CR (%)		5.7

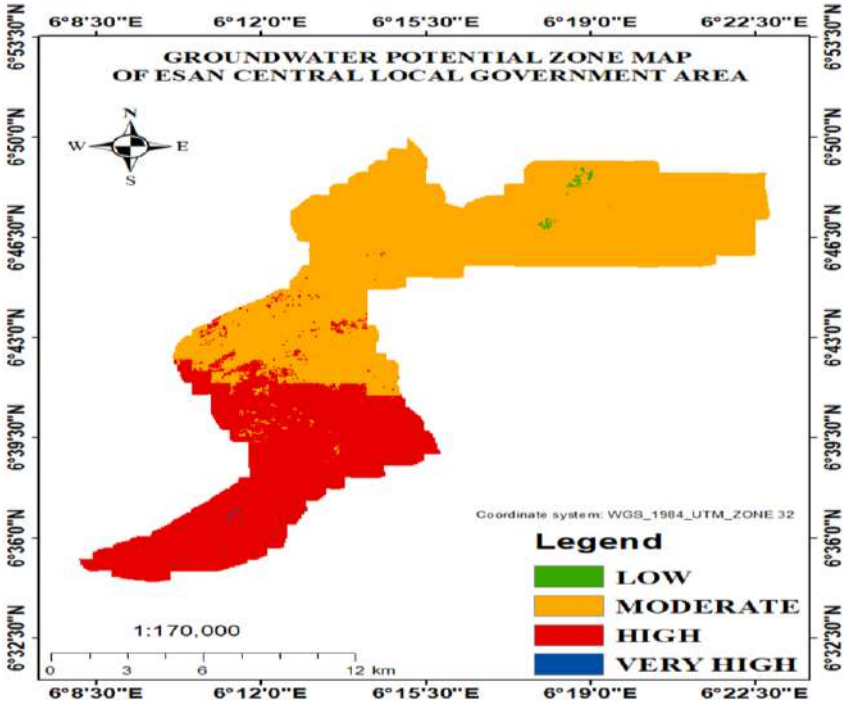

Figure 11: Groundwater Potential Zone Map

The integration of all thematic maps facilitated the delineation of groundwater potential zones in the study area. These zones are categorized into four classes: very high, high, moderate, and low. The low groundwater potential zone covers 0.506 km² of the study area, while the moderate potential zone covers 153.367 km². On the other hand, the high to very high groundwater potential zones cover 81.307 km² and 0.103 km², respectively, in the northern, central, and southern regions of the study area, as depicted in Figure 11.

Esan LGA is made up of about 26 main settlements, namely: Eko, Udowo, Eideru, Ewuh, Idua, Ibore, Irrua, Irrua STH, M.U., Oghagbo Opoji, Opoji, Ugbenolhua, Ididigba, Ewu monastery, Atuagbo, Ujabhole, Afuda, Ewu-Esan, Ugbalo, Idumoza, Ugbegun2, Ekekhen, Ugbegun, Ebudin S.S., Izogen,

DSHC. The Groundwater Potential Zone Map shows that areas with high groundwater potential are seven (7) locations, viz: Opoji, DSHC, Ugbegun2, Ekekhen, Ugbegun, Ebudin, and Izogen.

3.3 Results of Borehole Suitability Analysis

Due to their relevance to Water supply (that is, Borehole), six conditioning factors were selected for the spatial modelling. These are: Geological Condition, Soil Type, Distance to road network (m), Distance to residential areas (m), Elevation (m), and Slope.

3.3.1 Geological Condition

This represents the distribution of materials on or close to the Earth's surface. For this region of study, the geology of the place is found to have Quaternary eolian deposits of sand, clastic sediments of sedimentary rock called sandstone, and also clay. The sandstone area is the most demanding to drill through. The map of the Geological conditions of our study area is shown in Figure 12.

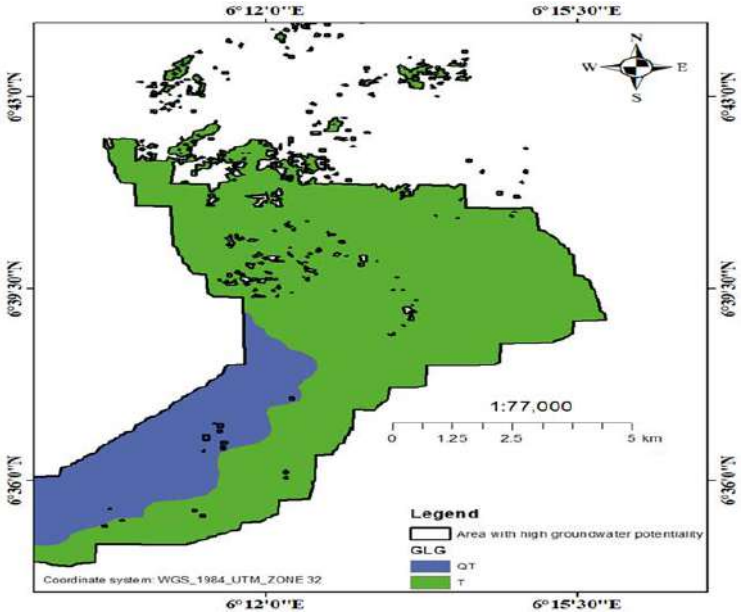

Figure 12: Geology map

3.3.2 Soil type

This refers to the porosity, permeability, drainage, and water-holding capacity of the soils. The map was generated from FAO soil data. This is regarded as the second most important factor. For this area of study, the soil types present are Clay and Loamy soil. 43 Loam soil is more permeable and less cohesive than clay, thus making loamy soil easier to drill through than clay soil. Clay soil has a high clay content and thus, more prone to sticking to drill bits or causing clogging during the drilling process. The soil map of the study area is shown in Figure 13.

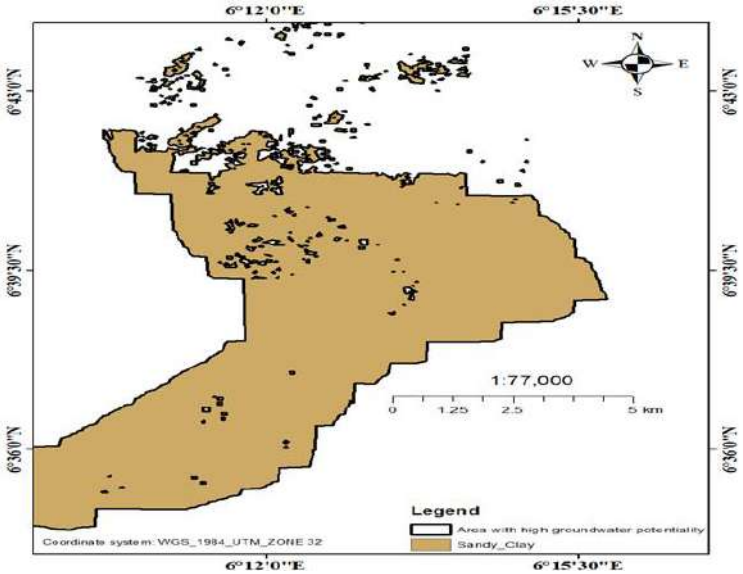

Figure13: Soil map

3.2.3 Distance to Road Network

Distance to road network map refers to the distance in meters from the borehole point to the nearest road. Close proximity to a road network facilitates access to the borehole for maintenance, repairs, and the transportation of drilling equipment. It can also simplify

the distribution of water to the surrounding communities. This factor is considered the third most important when siting a borehole. From Figure 14, 0 - 6.712 m indicates the area closest to the road.

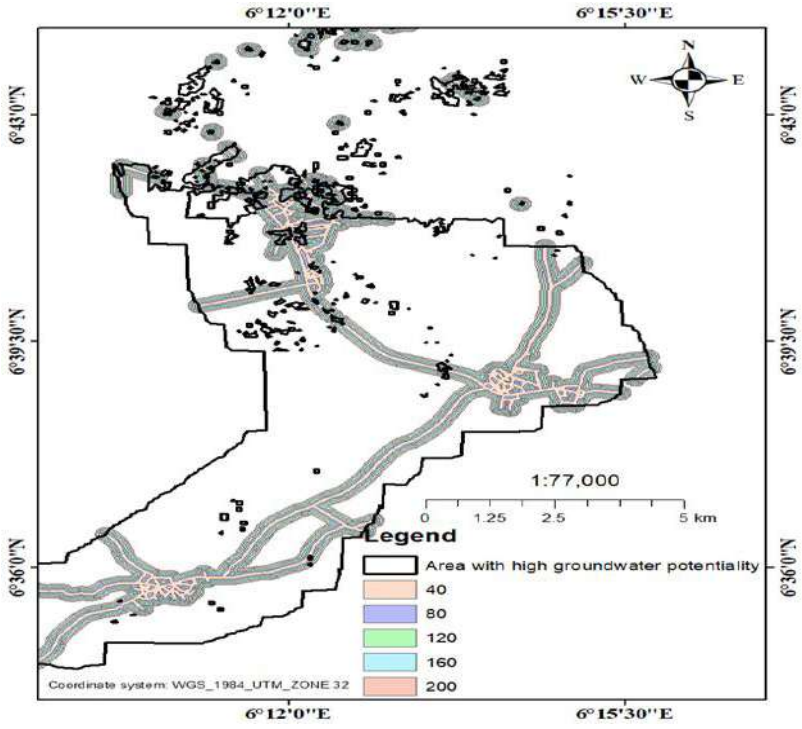

Figure14: Distance to road network map (buffered)

3.2.4 Distance to Residential Area

This is regarded as the fourth most important factor to be considered when sitting in a borehole. The distance to residential areas is important to ensure convenient access to the borehole for the community it serves. Reducing the distance helps minimize the effort required to collect water, especially for vulnerable populations, such as the elderly or children. The distance to residential areas map refers to the distance in meters from the point of the borehole to residences. From the distance map shown in Figure 15, 0 - 51.131 m indicates the region closest to the borehole.

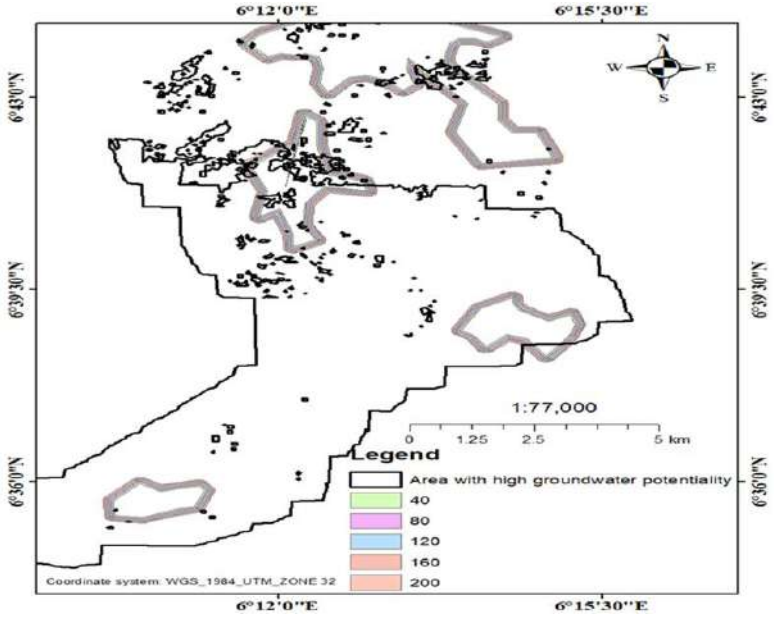

Figure 15: Distance to residential area map (buffered)

3.2.5 Elevation

Elevation plays a dual role in recharge potential and borehole construction logistics. The elevation in the study area was classified into five suitability categories. Lower elevations (135–227 m), which cover most of the central region, were rated the highest weight of (5), indicating favorable recharge and lower drilling costs. Conversely, elevations between 364–432 m received the lowest weight (1) due to potential runoff and logistical drilling challenges. These are found mainly in the northeastern margins of the study area. As shown in Figure 16

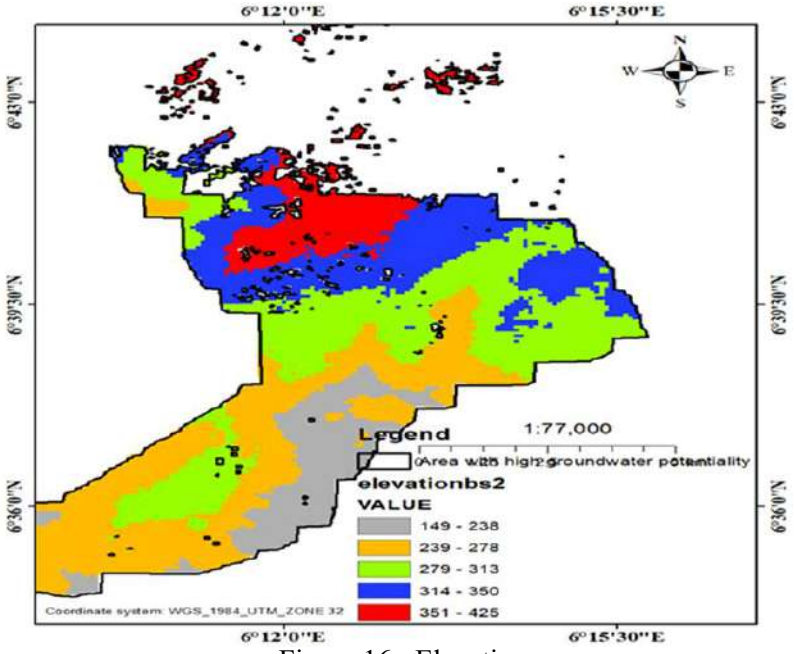

Figure 16: Elevation map

3.2.6 Slope

Slope strongly influences groundwater infiltration by controlling surface runoff rates. Table 8 shows that flat terrains (0°) received the highest suitability weight (5), indicating very high infiltration potential. These flat to gentle slopes dominate the southwestern and central regions of the study area, facilitating better infiltration and recharge due to slower water movement. In contrast, steep (89.948°–89.98°) and very steep slopes (89.981°–89.998°), with weights of 2 and 1, respectively, are concentrated in the northeast and are associated with high runoff and minimal recharge potential. This supports the inverse relationship between slope and groundwater suitability. Figure 17 is the resultant map showing the slope characteristics around the study area

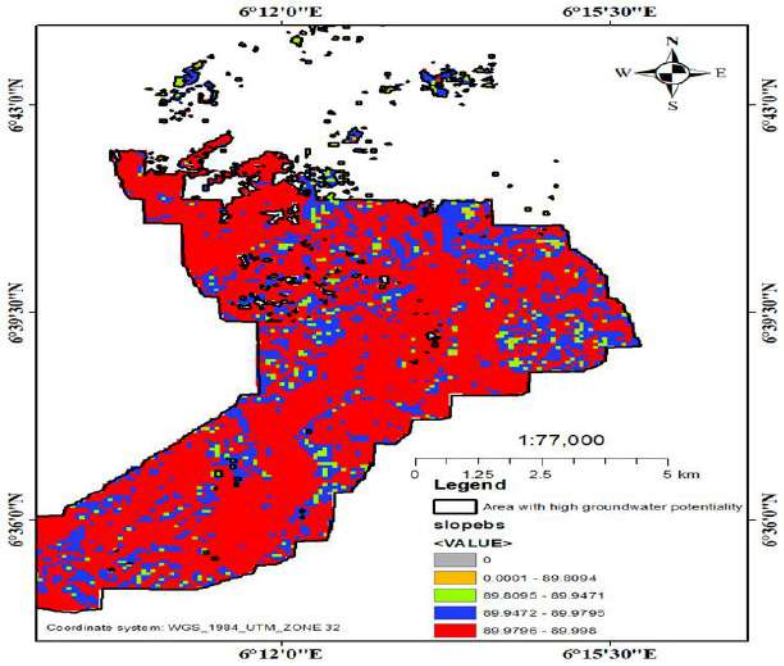

Figure 17: Slope map

3.3 Mapping of Borehole Siting Suitability Zones

The relative importance of the six criteria used in borehole suitability analysis, geology, soil type, distance to road network, distance to residential areas, elevation, and slope was determined using a 6×6 pairwise comparison matrix based on the Analytical Hierarchy Process (AHP). This process yielded a Consistency Ratio (CR) of 1.9%, which confirmed the reliability and logical consistency of the weighting scheme.

Geology and soil type were assigned the highest weights due to their dominant influence on aquifer potential and drilling feasibility. These were followed by proximity to roads and residential areas, which are critical for borehole accessibility and maintenance. Elevation and slope, though less influential, were also considered due to their effect on recharge dynamics and structural challenges during drilling. Figure 18 depicts

the final suitability map, which integrates these weighted criteria to identify optimal locations for borehole development across the study area. The most favorable zones are concentrated in the central corridor, where geological, infrastructural, and hydrological conditions align to support sustainable groundwater extraction.

Borehole siting factors were ranked using AHP based on their practical and hydrological significance. The consistency of the model ensured the reliability of the weighting scheme. Figure 18 depicts the most suitable sites, which align with favorable geological and infrastructural characteristics. These areas, mainly within the central corridor of the study area, offer ideal conditions for sustainable borehole development.

Table 8: Consistency ratio for Borehole Siting

N		**6**
λ_{max}	$\frac{(\lambda_{max}-n)}{n-1}$	
CI	$\frac{(6.122-6)}{6-1}$	0.024
RI		1.24
CR	CI/RI	0.019
CR (%)		1.9

The value of CR is less than 0.1, so we can say our AHP is consistent. The proportion of the study area classified as high groundwater potential (34.5%) is consistent with findings from similar studies across Africa. For example, [26] reported 28% high-potential zones in Ethiopia's Raya Valley, while [27] found in Turkana South, Kenya, that the lineaments found in the area correlate well with fault zones in a borehole assessment study. This similarity suggests a comparable hydrogeologic structure and supports the reliability of the model within tropical/sub-humid African environments.

3.4 Analysis of Borehole Siting Suitability Map

A ±10% sensitivity analysis was conducted to evaluate the robustness of the assigned AHP weights. We perturbed the weight of the top-ranking criterion (rainfall) by ±10%, and proportionally adjusted the others to maintain a sum of 1. The spatial extent of high and very high groundwater potential zones changed by less than 2%, indicating that the model's final output is stable and not overly sensitive to minor variations in judgmental weights [25]. This confirms the robustness of the AHP weight configuration used. Key factors like geology, soil, and road proximity remain fundamental to borehole suitability mapping [28]; [29]. This study demonstrates AHP's effectiveness while emphasizing the need for adaptable approaches to address data constraints and environmental variability. Table 9 shows the extract of the coordinates of the suitable locations for sitting a borehole within the study area.

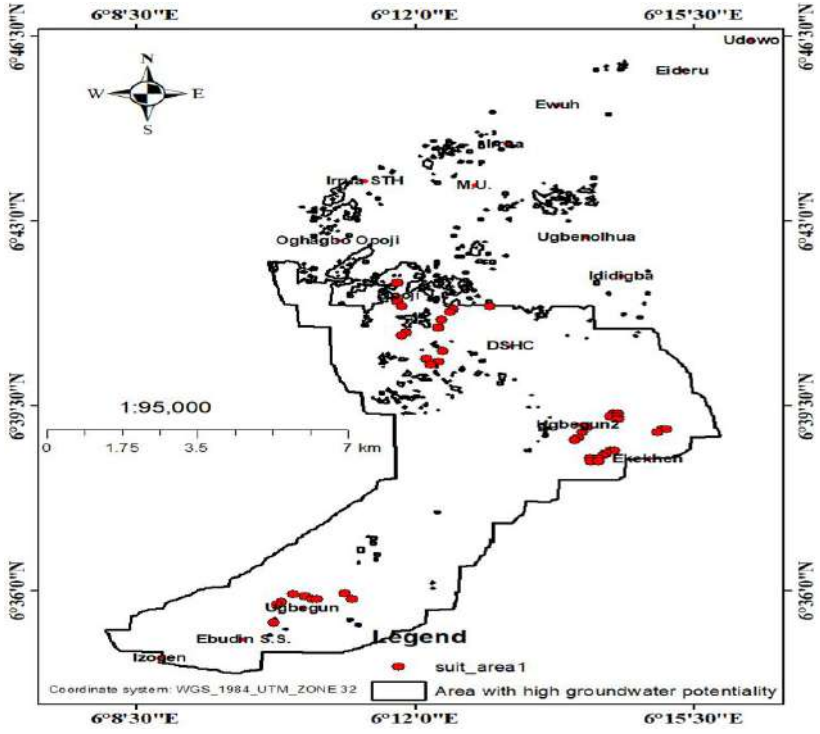

Figure 18: Borehole Siting Suitability Map

Table 9: Extract of coordinates of suitable sites

Point_ID	Eastings	Northings	Point_ID	Eastings	Northings	Point_ID	Eastings	Northings
1	190023	741156	16	195084	736555	31	194440	734991
2	190023	740512	17	194900	736463	32	194624	734991
3	190115	740328	18	195084	736463	33	194440	734899
4	192139	740328	19	195084	736371	34	194624	734899
5	191311	740236	20	194348	736095	35	187538	730297
6	191219	740144	21	196096	736003	36	188734	730297
7	191035	739868	22	196188	736003	37	187814	730205
8	190943	739592	23	194256	735911	38	187998	730113
9	190207	739408	24	196004	735911	39	188090	730113
10	190115	739316	25	194164	735727	40	188918	730113
11	191035	738764	26	194072	735635	41	187262	730021
12	190667	738487	27	194900	735267	42	187170	729929
13	190943	738395	28	194992	735267	43	187078	729285
14	190759	738303	29	194808	735175			
15	194992	736555	30	194716	735083			

Despite the model's overall reliability, there are limitations worth noting. The use of a 30-meter resolution DEM may obscure micro-topographic variations that influence localized recharge and runoff. Additionally, CRU rainfall data, while valuable for its spatial coverage, may not fully capture short-term precipitation variability or localized rainfall events, potentially affecting the precision of the recharge estimates. Future models can benefit from integrating higher-resolution topographic data such as LiDAR or Drone and locally calibrated rainfall datasets from meteorological stations or radar sources.

4. Conclusions

Throughout the project, a comprehensive analysis was undertaken to assess the groundwater potential of the study area. By integrating diverse geospatial datasets encompassing geological, hydrological, topographic, and climatic information, we successfully identified and delineated groundwater potential zones based on their suitability for both recharge and extraction. This study has found that groundwater potential and borehole siting in Esan Central LGA are strongly influenced by the synergy between geological, climatic, and infrastructural factors. The delineated high-potential zones offer a practical guide for optimizing resource allocation in water infrastructure projects. Future work should incorporate aquifer-depth modelling and groundwater quality assessments to enhance the reliability of borehole placement, especially in geologically diverse areas. Incorporating geophysical validation and seasonal variability analysis will also provide deeper insight into long-term water sustainability. The following are recommended: water resource planners should prioritize drilling in central Esan Central, particularly in communities such as Opoji, Ugbegun, Ekekhen, and Izogen for cost-effective borehole development directed towards amelioration water scarcity sufferings by the inhabitants. Community-scale boreholes in these zones could lower installation and maintenance costs by approximately 25% due to reduced drilling resistance and logistical efficiency. Edo State government should establish a regional groundwater monitoring framework will help track aquifer recharge rates, depth profiles, and seasonal variability, enabling more sustainable and data-driven water management decisions.

Acknowledgement

The authors wish to appreciate the organizations and individuals who have provided us with all the relevant information and data such as: Glovis, USGS, FAO.

References

[1] N. Carrard, T. Foster, and J. Willetts, "Groundwater as a source of drinking water in Southeast Asia and the Pacific: A multi-country review of current reliance and resource concerns," *Water*, vol. 11, no. 8, p. 1605, Aug. 2019, doi: 10.3390/w11081605.

[2] M. O. Eyankware, E. O. Igwe, C. Ogwah, and R. O. E. Ulakpa, "Achieving sustainable use and management of water resources for irrigation in Nigeria," *J. Environ. Earth Sci.*, vol. 2, no. 2, pp. 47–55, 2020, doi: 10.30564/jees.v2i2.2505.

[3] Y. Aranguren-Díaz et al., "Aquifers and groundwater: Challenges and opportunities in water resource management in Colombia," *Water*, vol. 16, no. 5, p. 685, Mar. 2024, doi: 10.3390/w16050685.

[4] V. Sheel et al., "Water as a social determinant of health: Bringing policies into action," J. Glob.

Health Rep., vol. 8, p. e2024003, 2024, doi: 10.29392/001c.92160.
[5] P. Ekins and D. Zenghelis, "The costs and benefits of environmental sustainability," *Sustain. Sci.*, vol. 16, pp. 949–965, 2021, doi: 10.1007/s11625-021-00910-5.
[6] R. Agarwal and P. K. Garg, "Remote sensing and GIS based groundwater potential & recharge zones mapping using multi-criteria decision making technique," *Water Resour. Manag.*, vol. 30, no. 1, pp. 243–260, Jan. 2016, doi: 10.1007/s11269-015-1159-8.
[7] P. A. Opoku, L. Shu, and G. K. Amoako-Nimako, "Assessment of groundwater potential zones by integrating hydrogeological data, geographic information systems, remote sensing, and analytical hierarchical process techniques in the Jinan karst spring basin of China," *Water*, vol. 16, no. 4, p. 566, Feb. 2024, doi: 10.3390/w16040566.
[8] O. G. Bayowa et al., "Integration of hydrogeophysical and remote sensing data in the assessment of groundwater potential of the basement complex terrain of Ekiti State, Southwestern Nigeria," *Ife J. Sci.*, vol. 18, no. 1, pp. 353–363, 2016.
[9] K. S. Ishola et al., "Groundwater potential mapping in hard rock terrain using remote sensing, geospatial and aeromagnetic data," *Geosyst. Geoenv.*, vol. 2, no. 1, p. 100107, 2023, doi: 10.1016/j.geogeo.2022.100107.
[10] M. A. Hussein, M. Y. Ali, and H. A. Hussein, "Groundwater investigation through electrical resistivity tomography in the Galhareri district, Galgaduud region, Somalia: Insights into hydrogeological properties," *Water*, vol. 15, no. 18, p. 3317, Sep. 2023, doi: 10.3390/w15183317.
[11] S. T. Owolabi et al., "A groundwater potential zone mapping approach for semi-arid environments using remote sensing (RS), geographic information system (GIS), and analytical hierarchical process (AHP) techniques: A case study of Buffalo catchment, Eastern Cape, South Africa," *Arab J. Geosci.*, vol. 13, p. 1184, 2020, doi: 10.1007/s12517-020-06166-0.
[12] T. L. Saaty, The Analytic Hierarchy Process: Planning, Priority Setting, Resource Allocation. New York, NY, USA: McGraw-Hill, 1980.
[13] T. L. Saaty, "Decision making with the analytic hierarchy process," *Int. J. Serv. Sci.*, vol. 1, p. 83, 2008, doi: 10.1504/IJSSCI.2008.017590.
[14] J. O. Osumeje et al., "Application of remote sensing and electrical resistivity technique for delineating groundwater potential in North Western Nigeria," Sci. Rep., vol. 14, no. 1, p. 22299, 2024, doi: 10.1038/s41598-024-69633-8.
[15] A. D. Mangs et al., "Groundwater potential mapping in Lapan Gwari community using integrated remote sensing and electrical resistivity soundings," *Int. J. Geosci.*, vol. 14, pp. 719–732, 2023, doi: 10.4236/ijg.2023.148039.
[16] T. Kumar, A. K. Gautam, and T. Kumar, "Appraising the accuracy of GIS-based multicriteria decision making technique for delineation of groundwater potential zones," *Water Resour. Manag.*, vol. 28, no. 13, pp. 4449–4466, Oct. 2014, doi: 10.1007/s11269-014-0663-6.
[17] M. M. Tshanga, L. Ncube, and E. van Niekerk, "Remote sensing insights into subsurface-surface relationships: Land cover analysis and copper deposits exploration," Earth Sci. Inform., vol. 17, pp. 3979–4000, 2024, doi: 10.1007/s12145-024-01423-2.
[18] L. Ramasubramanian, "Book review: Wade, T., and S. Sommer, eds. 2006. A to Z GIS: An illustrated dictionary of geographic information systems. Redlands, CA: ESRI Press," *J. Plan. Lit.,* vol. 23, no. 3, pp. 263–264, 2009, doi: 10.1177/0885412208327016.
[19] A. A. Woldegebriel, T. A. Amibo, and A. B. Bayu, "Evaluation of groundwater potential zone using remote sensing and geographical information system: In Kaffa zone, South Western Ethiopia," Appl. Water Sci., vol. 11, p. 41, 2021, doi: 10.1007/s13201-020-01308-2.
[20] N. E. Okello et al., "Assessment of groundwater recharge potential in semi-arid regions using remote sensing and GIS techniques: A case study of Laikipia County, Kenya," *Environ. Dev. Sustain.*, vol. 22, pp. 1369–1386, 2020, doi: 10.1007/s10668-018-0300-z.
[21] A. K. Singh, M. K. Singh, and S. K. Singh, "Groundwater potential zone mapping using GIS and remote sensing techniques: A case study in Siwan district, Bihar, India," *Arab J. Geosci.*, vol. 13, p. 568, 2020, doi: 10.1007/s12517-020-05319-1.
[22] D. N. Chavan et al., "GIS based groundwater potential zone mapping in semiarid region of Maharashtra, India," Environ. Monit. Assess., vol. 192, p. 597, 2020, doi: 10.1007/s10661-020-08674-y.
[23] R. S. Raju, G. S. Raju, and M. Rajasekhar, "Identification of groundwater potential zones in Mandavi River basin, Andhra Pradesh, India using remote sensing, GIS and MIF techniques," *HydroResearch*, vol. 2, pp. 1–11, 2019, doi: 10.1016/j.hydres.2019.09.001.
[24] A. Y. Khan et al., "Integrated geophysical and geospatial techniques for surface and groundwater modeling," *Sci. Rep.*, vol. 14, no. 1, p. 25514, 2024, doi: 10.1038/s41598-024-76262-8.
[25] R. Gupta and A. Anshumali, "Groundwater potential zone mapping using remote sensing and GIS techniques: A case study of the Kharun River

Basin, India," *Arab J. Geosci*., vol. 14, p. 1864, 2021, doi: 10.1007/s12517-021-08232-3.

[26] A. A. Fenta et al., "Spatial analysis of groundwater potential using remote sensing and GIS-based multi-criteria evaluation in Raya Valley, northern Ethiopia," *Hydrogeol. J*., vol. 23, no. 1, pp. 195–206, 2015.

[27] D. Nyaberi et al., "Groundwater resource mapping through the integration of geology, remote sensing, geographical information systems and borehole data in arid-subarid lands at Turkana South Sub-County, Kenya," *J. Geosci. Environ. Prot*., vol. 7, pp. 53–72, 2019, doi: 10.4236/gep.2019.712004.

[28] S. M. Ibrahim et al., "Remote sensing and GIS techniques in groundwater potential zone mapping: A case study in Northern Iraq," *Geocarto Int*., vol. 35, no. 4, pp. 407–428, 2020, doi: 10.1080/10106049.2018.1492525.

[29] K. M. Nnaji, S. O. Aladesanmi, and A. O. Ojo, "Groundwater potential mapping using remote sensing and GIS: A case study of Akure, Southwestern Nigeria," *Environ. Earth Sci*., vol. 77, no. 19, p. 654, 2018, doi: 10.1007/s12665-018-7899-z.